

Collective dynamics in dense Hg vapour

This article has been downloaded from IOPscience. Please scroll down to see the full text article.

2004 J. Phys.: Condens. Matter 16 L45

(<http://iopscience.iop.org/0953-8984/16/6/L03>)

View [the table of contents for this issue](#), or go to the [journal homepage](#) for more

Download details:

IP Address: 129.252.86.83

The article was downloaded on 27/05/2010 at 12:39

Please note that [terms and conditions apply](#).

LETTER TO THE EDITOR

Collective dynamics in dense Hg vapour**D Ishikawa^{1,4}, M Inui², K Matsuda¹, K Tamura¹, A Q R Baron³,
S Tsutsui³, Y Tanaka⁴ and T Ishikawa^{3,4}**¹ Graduate School of Engineering, Kyoto University, Kyoto, 606-8501, Japan² Faculty of Integrated Arts and Sciences, Hiroshima University,
Higashi-Hiroshima 739-8521, Japan³ SPring-8/JASRI 1-1-1 Kouto, Mikazuki-cho, Sayo-gun, Hyogo-ken, 679-5198, Japan⁴ SPring-8/RIKEN 1-1-1 Kouto, Mikazuki-cho, Sayo-gun, Hyogo-ken, 679-5148, Japan

Received 17 November 2003

Published 30 January 2004

Online at stacks.iop.org/JPhysCM/16/L45 (DOI: 10.1088/0953-8984/16/6/L03)**Abstract**

The dynamic structure factor, $S(Q, \omega)$, of dense Hg vapour has been measured by high resolution inelastic x-ray scattering for densities of 3.0, 2.1 and 1.0 g cm⁻³ corresponding to 0.52, 0.36 and 0.17 times the critical density, respectively, and for momentum transfers between 2.0 and 48 nm⁻¹. Analysis of the longitudinal current–current correlation function in the framework of generalized hydrodynamics reveals that the frequencies of the collective excitations increase faster with Q than estimated from the macroscopic speed of sound. The ratios of the frequencies were found to be 1.27 at 3.0 g cm⁻³, 1.12 at 2.1 g cm⁻³ and 1.10 at 1.0 g cm⁻³. The sound velocity obtained from the present experiments is well reproduced by a wavenumber dependent adiabatic sound velocity, which means that the collective modes remain in the spectra of dense Hg vapour.

A substantial and continuous volume expansion from the liquid to the rarefied vapour occurs by a change of the temperature and pressure surrounding the liquid–vapour critical point, without crossing the saturated vapour pressure curve. In the expansion process, the mean interatomic distance increases up to ten times that under normal conditions. Physical properties of metallic fluids, in contrast to those of molecular fluids, are dramatically changed. A review of expanded fluid metals may be found in the literature [1]. Liquid Hg is well known as a prototype of liquid metals, and has been extensively investigated because it has the lowest critical temperature among liquid metals. Liquid Hg is transformed into an insulating state around 9 g cm⁻³ when it is expanded to the liquid–gas critical point (critical data of Hg [2]: $T_C = 1478$ °C, $P_C = 1673$ bar, $\rho_C = 5.8$ g cm⁻³).

It is interesting to study the vapour phase of fluid Hg because Hg vapour is the state before it is condensed to the metallic state. In the vapour phase of Hg, chemically bonded dimers were not considered to form because the ground state of the Hg atom arises from a closed shell electronic configuration which cannot form an appreciable bond owing to the inert character

of the $6s^2$ shell. The interaction potential between two Hg atoms used to be regarded as acting between highly polarizable closed-shell systems, involving very little electronic density migration from the partners, in a similar way to noble gas atoms. In this sense, Hg vapour has been called 'pseudo-helium' [3]. Contrary to this common-sense view, however, the formation of Hg dimers has recently been pointed out. The ground state bond length of the gas phase Hg_2 was, in fact, determined by taking high resolution spectra of an isotopically selective vibronic band of the jet-cooled molecule [4]. Measurements of optical absorption spectra [5] and depolarized interaction-induced light scattering spectroscopy (DILS) [6–8] also suggest that there exist dimers in the Hg vapour. Recently x-ray diffraction measurements [9] for dense Hg vapour were successfully carried out and, by analysing the obtained static structure factor, $S(Q)$, the interatomic distance in the dense vapour was found to be close to that of an Hg dimer. It is evident that in addition to the static structure the investigation of dynamic structure in Hg vapour is important. An inelastic x-ray scattering (IXS) technique using the third generation source of synchrotron radiation is a useful probe to study the collective excitation and single particle behaviour.

In this letter, we report the dynamic structure factor, $S(Q, \omega)$, of Hg vapour at high temperatures of 1150, 1350, and 1450 °C and pressures of 510, 1023 and 1398 bar. IXS allows us to overcome the kinematic limitations of neutron scattering and, furthermore, provides a small spot size (about 0.1 mm in diameter) facilitating the use of extreme sample environments. While the high atomic number of Hg and therefore the relatively small ratio of scattering to absorption for x-rays makes this experiment difficult, we have succeeded in obtaining good quality data.

This work has been done at the high-resolution IXS beamline (BL35XU) of SPring-8 in Japan [10]. Backscattering at the Si(11 11 11) reflection was used to provide a beam of 3×10^9 photons s^{-1} in a 0.8 meV bandwidth onto the sample. The energy of the incident beam and the Bragg angle of the backscattering were 21.747 keV and 89.98°, respectively. We used three spherical analyser crystals at the end of the 10 m horizontal arm to analyse the scattered x-rays. The spectrometer resolution was 1.7–1.8 meV. Note that the resolution was slightly degraded compared to the best one because our large high-pressure vessel forced the detectors about 240 mm away from the sample position. The momentum resolution was 1 nm^{-1} , corresponding to the 95 mm diameter of the analysers at the 9.8 m radius.

The Hg sample of 99.999% purity and 100 μm thickness was mounted in a single-crystal sapphire cell [11] and He gas of 99.9999% purity was used as a pressurizing medium. The high-pressure vessel, which can be operated up to 1700 °C and 2000 bar, had small Be windows of 10 mm in diameter and 10 mm in thickness which allowed us to measure at discrete scattering angles of 2θ of 1°, 5°, 10°, 19° and 24°. In each case the window aperture allowed the use of three analyser crystals, so we have data at 15 momentum transfers from 2.0 to 48.3 nm^{-1} .

Measurements were made for three different densities, ρ , of 3.0, 2.1 and 1.0 g cm^{-3} . Their corresponding temperatures and pressures are $T = 1450, 1350$ and 1150 °C and $P = 1398, 1023$ and 510 bar, respectively. He gas contributed significant background, especially at low momentum transfers, where the intensity of the background was comparable to that of the signal. Thus backgrounds were measured at each pressure and temperature, and were subtracted after being scaled for sample transmission.

Selected IXS data at $\rho = 3.0 \text{ g cm}^{-3}$ are shown in figure 1. The integral, $I(Q)$ of the spectrum, $I(Q, \omega)$, was calculated, and was used for the normalization, so $I(Q, \omega)/I(Q)$ is plotted in the figure. The resolution function obtained from a measurement of a PMMA (polymethyl-methacrylate) is shown by a broken curve at the bottom on the left. The IXS spectra have a single peak and the line width of the peak (FWHM) becomes large with increasing Q . The line shapes at the other densities were similar to those at 3.0 g cm^{-3} .

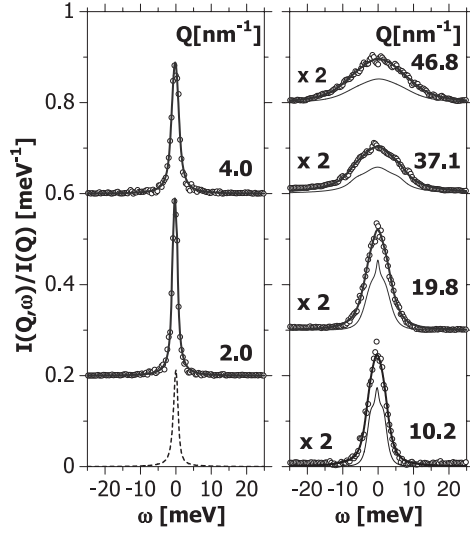


Figure 1. IXS spectra (open circles) of dense Hg vapour at $\rho = 3 \text{ g cm}^{-3}$ ($\rho = 0.52\rho_C$, $T = 1450 \text{ }^\circ\text{C}$ and $P = 1398 \text{ bar}$) after background subtraction. The experimental data are normalized to their integrated intensity and fits (solid curves) were made by convoluting the resolution function (dashed curve) to a model function, a Lorentzian plus damped harmonic oscillator model. The thin solid curve denotes the optimized model function free from the resolution of the spectrometer. IXS spectra from 10.2 to 46.8 nm^{-1} are multiplied by two.

We analysed the data in the framework of generalized hydrodynamics [12]. As shown in figure 1, the observed spectra have a single peak without a side-peak or a shoulder revealing a collective excitation. Since $S(Q, \omega)$ without clear evidence of a collective mode was first observed for classical liquids such as liquid Ar, it has been discussed whether the sound mode with wavelength less than the interatomic distance would be meaningful or not. de Schepper *et al* [13], and McGreevy and Mitchell [14] discussed strongly damped sound waves of liquid Ar and insisted on the existence of the sound mode. In addition, this model has been used with great success in many experiments on liquids. Based on these discussions we assume that the present spectra at low momentum transfer have a component of a collective excitation. Then the present IXS spectra were modelled as the sum of Lorentzian at zero energy transfer, representing the thermal contribution, and a damped harmonic oscillator [15] for the sound mode with the statistical occupation factor according to equation (1). Note that this model function was the same one used for the analysis of liquid Ar [13]:

$$S(Q, \omega)/S(Q) = \frac{\beta\hbar\omega}{1 - \exp(-\beta\hbar\omega)} \left[\frac{A_0}{\pi\Gamma_0} \frac{\Gamma_0^2}{\omega^2 + \Gamma_0^2} + \frac{A_Q}{2\pi\Gamma_Q} \frac{4\omega_Q\Gamma_Q^2}{(\omega^2 - \Omega_Q^2)^2 + 4\omega^2\Gamma_Q^2} \right] \quad (1)$$

where $\beta = (k_B T)^{-1}$ and $\omega_Q = \sqrt{\Omega_Q^2 - \Gamma_Q^2}$. The parameters A_0 and Γ_0 are the magnitude and FWHM of a quasi-elastic peak, while A_Q , Ω_Q , and Γ_Q are the magnitude, energy and width of inelastic excitations. We optimized these parameters by convoluting the model function with the measured resolution function and fitting to the data. The optimized model function is also plotted in figure 1 by a thin solid curve. There appears a clear shoulder in the optimized model function at 10.2, 19.8 and 37.1 nm^{-1} . The position is almost coincident with Ω_Q and the error of Ω_Q is within $\pm 10\%$. Details of the optimized parameters will be discussed elsewhere.

As shown in figure 1, the line shape of the spectra in Q at 2.0–4.0 nm^{-1} is almost the same as that of the resolution functions, so it was difficult to deduce deconvoluted spectra.

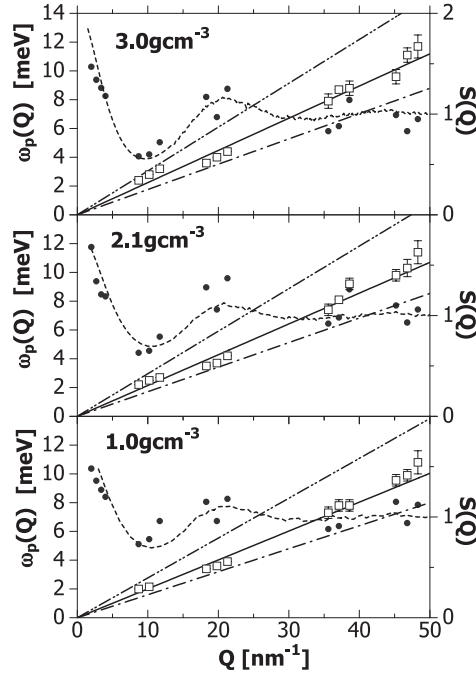


Figure 2. The peak of the current–current correlation function (squares) as a function of Q at densities of 3.0, 2.1 and 1.0 g cm^{-3} . Solid lines correspond to the low- Q limit of the sound velocity [16, 17]. Dotted curves, dash-dotted lines and dash-double-dotted lines are the static structure factor, $S(Q)$, [9], isothermal frequency, ω_0 , and ideal-gas limit, ω_L^{ig} , respectively. Closed circles show $I(Q)$ normalized by the square of the atomic form factor and polarization factor.

In the intermediate Q region around 10–20 nm^{-1} , the line shapes become broad and the fitting procedure could be applied. In the large Q region from 37 to 48 nm^{-1} , the line shapes become much broader than those around 2.0–4.0 nm^{-1} . In this region the central peak is expected to shift towards positive energy side by the recoil. However, due to the large mass of an Hg atom, a small recoil energy shift $\omega_R = \hbar^2 Q^2 / 2m$ which is estimated to be 0.23 meV at 46.8 nm^{-1} could not be observed within the statistical errors.

The model function was used to determine the longitudinal current–current correlation function, $J_\ell(Q, \omega)$, expressed by

$$J_\ell(Q, \omega) = \frac{\omega^2}{Q^2} S(Q, \omega). \quad (2)$$

The maximum of $J_\ell(Q, \omega)$ is considered to give a characteristic frequency ω_p relating the sound velocity. Figure 2 shows the Q dependence of ω_p (squares) for each density together with the static structure factor $S(Q)$ (dotted curves) measured by x-ray diffraction [9], and sound velocity (solid lines) obtained by the ultrasonic measurements [16, 17]. Also shown are the lower and upper limits for an ideal gas, which are isothermal energy $\omega_0 = (\beta m)^{-1/2} Q$ (dash-dotted lines) and thermal energy of a single atom $\omega_L^{\text{ig}} = (\beta m / 3)^{-1/2} Q$ (dash-double-dotted lines). Closed circles in the figure denote properly normalized $I(Q)$ to monitor counts with corrections for polarization and x-ray form factor, and they seem to agree nicely with $S(Q)$ from previous work [9]. Note that $S(Q)$ at 1.0 g cm^{-3} was not available but we use our preliminary results obtained by x-ray diffraction. The plots of ω_p are almost arranged along

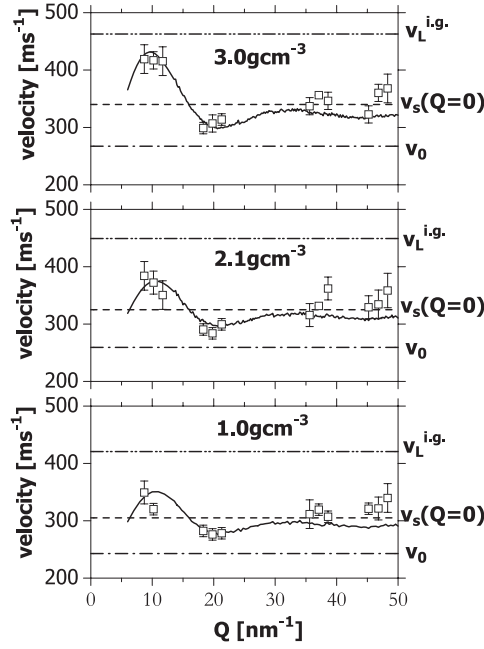


Figure 3. The effective velocity $\omega_p(Q)/Q$, in dense Hg vapour at 3.0, 2.1 and 1.0 g cm^{-3} (squares), and the sound velocity [16, 17] (broken lines). Also shown are the isothermal velocity, v_0 , (dash-dotted lines), average thermal velocity of a single atom, $v_L^{\text{i.g.}}$ (dash-double-dotted lines) and wavenumber dependent adiabatic velocity, $v_s(Q)$, (solid curves) with $\gamma \sim 1.4$ (see text).

the line denoting the sound velocity up to the high Q region. In detail, ω_p around 10 nm^{-1} deviates positively from the line. The amount of positive deviation is estimated to be 27% at 3.0 g cm^{-3} , 12% at 2.1 g cm^{-3} and 10% at 1.0 g cm^{-3} . This behaviour is similar to the positive dispersion observed in several liquids [18].

The region around 20 nm^{-1} corresponds to that near the first structure factor maximum, Q_m of $S(Q)$. The ω_p around 20 nm^{-1} is below the macroscopic value. The plots of ω_p seem to oscillate along the line. To see the behaviour of the oscillation, we plot the effective velocity, $v(Q) = \omega_p(Q)/Q$ (squares) in figure 3. Figure 3 also shows a wavenumber dependent adiabatic sound velocity $v_s(Q)$, given by

$$v_s(Q) = \sqrt{\frac{\gamma k_B T}{m S(Q)}}, \quad (3)$$

where m is the mass of a particle and γ is the specific-heat ratio (C_p/C_v). We neglect the Q dependence of γ , and estimated a reasonable value γ to fit $v_s(Q)$ to $v(Q)$. The curve of $v_s(Q)$ agrees reasonably with the experimental results up to 40 nm^{-1} if γ is assumed to be 1.4–1.5. The values of γ are calculated to be 1.67 and 1.4 for monatomic and diatomic ideal gases, respectively. Our estimation for γ is close to the diatomic value. This result hints that the dimer mode present in the gas phase.

In summary, we have measured the dynamic structure factor of compressed Hg vapour for $\rho/\rho_C = 0.52, 0.36$ and 0.17 , at high temperature and high pressure. In the dense gas phase, we have shown that the sound velocity obtained from the present experiments is well reproduced by a wavenumber dependent adiabatic sound velocity, $v_s(Q)$, which means that the collective modes remain in the spectra without any shoulder or side-peak observed for the Hg vapour.

The present result that γ is close to the diatomic value is consistent with other results [5–8] which suggests that the interaction in the vapour is different from the simple binary collisions dominant in noble gases. Additional experiments are under way to employ this technique over a wide density range from ambient conditions ($\rho/\rho_C = 2.3$), along the liquid–gas coexistence line and into the super-critical region.

The authors would like to thank Professor K Hoshino, Professor F Shimojo and S Tanaka for their valuable discussion. The authors acknowledge Dr K Tanaka, H Itoh, Y Itoh, K Satoh, K Mifune, M Kusakari, Y Naitoh and M Muranaka for their experimental support. Kobe Steel Co. Ltd and High Pressure System Co. Ltd are acknowledged for their technical support. This work is supported by the Grant-in-Aid for Specially Promoted Research from the Ministry of Education, Science and Culture of Japan under contract No. 11102004. The synchrotron radiation experiments were performed at the SPring-8 with the approval of the Japan Synchrotron Radiation Research Institute (JASRI) (Proposal No. 2003A6607-LD-np and 2003B0206-ND3d-np).

References

- [1] Hensel F and Warren W W Jr 1999 *Fluid Metals* (Princeton, NJ: Princeton University Press) and references therein
- [2] Gözlaff W, Schönherr G and Hensel F 1988 *Z. Phys. Chem. NF* **156** 219
- [3] Pyykkö P 1978 *Adv. Quantum Chem.* **11** 353
- [4] van Zee R D, Blankespoor S C and Zwier T S 1988 *J. Chem. Phys.* **88** 4650
- [5] Yao M, Hayami W and Endo H 1990 *J. Non-Cryst. Solids* **117/118** 473
- [6] Bonechi A, Barocchi F, Moraldi M, Bierman C, Winter R and Frommhold L 1998 *Phys. Rev. A* **57** 2635
- [7] Barocchi F, Hensel F and Sampoli M 1995 *Chem. Phys. Lett.* **232** 445
- [8] Sampoli M, Barocchi F, Guasti A, Winter R, Rathenow J and Hensel F 1992 *Phys. Rev. A* **45** 6910
- [9] Inui M, Hong X and Tamura K 2003 *Phys. Rev. B* **68** 094108
- [10] Baron A, Tanaka Y, Miwa D, Ishikawa D, Mochizuki T, Takeshita K, Goto S, Matsushita T, Kimura H, Yamamoto F and Ishikawa T 2001 *Nucl. Instrum. Methods A* **467/468** 627
- [11] Tamura K, Inui M and Hosokawa S 1999 *Rev. Sci. Instrum.* **70** 144
- [12] Boon J P and Yip S 1980 *Molecular Hydrodynamics* (New York: McGraw-Hill) and references therein
- [13] de Schepper I M, Verkerk P, van Well A A and de Graaf L A 1982 *Phys. Rev. Lett.* **50** 974
- [14] McGreevy R L and Mitchell E W J 1985 *Phys. Rev. Lett.* **55** 398
- [15] Fåk B and Dorner B 1992 *Institute Laue-Langevin Report* 92FA008S
- [16] Yao M, Okada K, Aoki T and Endo H 1996 *J. Non-Cryst. Solids* **205–207** 274
- [17] Okada K, Odawara A and Yao M 1998 *Rev. High Pressure Sci. Technol.* **7** 736
- [18] Morkel C, Bodensteiner T and Gemperlin H 1993 *Phys. Rev. E* **47** 2575